Short granular chain under vibration: multiple states and spontaneous switching

Y.-C. Sun[2], H.-T. Fei[1], P.-C. Huang[3], W.-T. Juan[1], J.-R. Huang[2,†] and J.-C. Tsai[1,*]
[1] *Institute of Physics, Academia Sinica, Taipei, Taiwan 11529*
[2] *Department of Physics, Nat'l Taiwan Normal University and*
[3] *Department of Physics, Nat'l Taiwan University*
(Dated: 2015.06.17+.GPT-2015states-jc0625c.tex)

We study experimentally a short chain of N($\leq$8) loosely connected spheres bouncing against a horizontal surface undergoing vertical vibrations of intensity Γ. Distinct states are identified and, depending on Γ, the response of the chain can be dominated by a base state of uniform bouncing in-sync with the substrate, or by more excited states with significant swinging of its end(s). In a transitional window of Γ, the spontaneous switching of states demonstrates a bi-stability that explains why qualitatively different bouncing modes can occur at the same initial position along a gradient of vibration we have reported previously in Phys. Rev. Lett. 112, 058001 (2014). Our high-speed tracking of individual particles measures their trajectories and energies along with the bifurcation of states and, on the other hand, the transitions over various factors are characterized by long-time statistics. Comparing our measurements to parabolic flights of a hypothetical point mass leads to basic understanding of the transition, while extended observations provide specific targets for further theoretical investigations. These studies help elucidate how the internal state of a soft dissipative object responds to external driving and affects its macroscopic motion.

I. INTRODUCTION

Response of granular objects to mechanical vibrations has brought a long tradition of scholarly works [1-10]. By convention, the vibration intensity Γ is specified by the peak acceleration of the substrate, normalized by the gravity g. Many studies have inspected the change of states or bouncing modes, in particular the dynamics of rigid objects. For instance, an early work by Sano and coworkers has addressed the occurrence of directional motion (referred to as a disorder-to-order transition) of an asymmetrical object at $\Gamma \approx 1.8$ [1]. The joint works by Kudrolli, Volfson, Tsimring, and their collaborators have discussed the re-bounce of dumbbells on a substrate at values of Γ slightly lower than 1 and the different bouncing modes that are presumably sensitive to initial conditions [2]. Wright, Swift, and King have studied numerically the state of a single ball on a concave vibrating surface and its dependence on the curvature [5]. A very recent paper by Kubo et al. combines experiments, simulations and analytical works on the bifurcations of bouncing modes that are coupled with the chirality of the object [9]. However, the response of a flexible object, i.e. those with internal degrees of freedom, are relatively less discussed.

In our previous experiments along a spatial gradient of vibration intensity [11], we use a short chain like other previous studies [10] as a generic representation of a soft, dissipative object, and discover an intriguing transition over the change of Γ: the dramatic spatial divide further illustrates the consequence of the transition when combined with the spatial asymmetry imposed by the gradient. It is interesting to note that, within a certain window of vibration intensity, the chain can choose its response stochastically from multiple available states. In our current work, we systematically study these transitions with a tunable intensity of vibration that is spatially uniform. The combination of microscopic and statistical analyses allows us to fully characterize different states of chain, and provides details that are essential for in-depth understanding of the transitions.

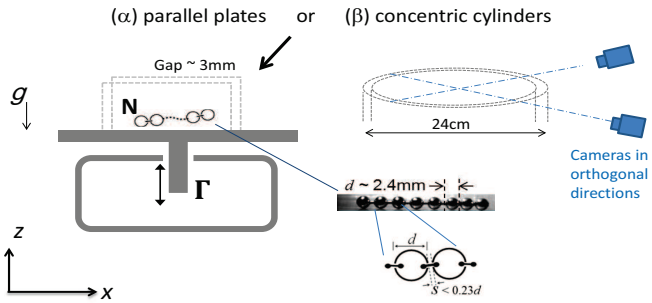

FIG. 1. Schematics of experimental setups and key dimensions of the objects.

II. SETUP AND AN OVERVIEW

As shown by Fig. 1, we impose sinusoidal vibrations with dimensionless intensity Γ to a chain of N loosely connected metal spheres (illustrated by the inset photograph and a schematic sketch). Our mechanical shakers are built by a local manufacturer (Vibration Source Technology, Co. Ltd., Taipei, Taiwan) and are feedback-controlled. The chain is partially confined by either (α) two acrylic plates with a separation slightly larger than the particle diameter d, or (β) concentric cylinders with the same gap width. The bottom of the channel is also made of acrylic but roughened at the scale of 0.1mm. In the linear version, the bottom is either (α1) flat with a total length about 30cm or (α2) slightly concave with a

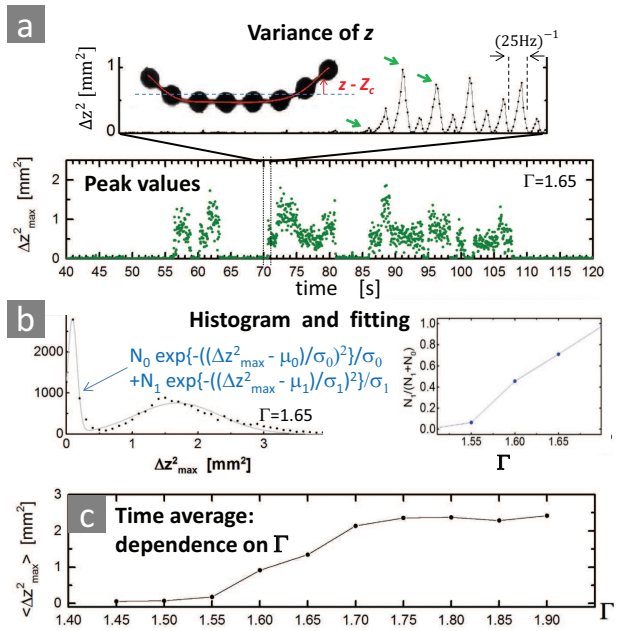

FIG. 2. Overview of the transition – **(a)** Spontaneous switch between the inactive state and the excited state(s) at a fixed value of Γ =1.65, as is indicated by the time evolution of the *peak values* in $\Delta z^2(t) \equiv \int (z - Z_c)^2 dx / \int dx$. The symbol Z_C stands for the height of the geometric center of the chain. **(b)** Histogram of the peak values with a bimodal fitting at Γ=1.65, and the fraction $N_1/(N_0 + N_1)$ as a function of Γ. **(c)** Time average of the peak values as a function of Γ. Experiments are performed at 25Hz with $N = 8$, setup $\alpha 1$ with images captured at 500fps over 18000 vibrations in each case.

radius of curvature about 20cm, depending on the purpose of measurements. In all experiments, the chain is illuminated by diffusive back lighting, with its images captured from the front view and, in the circular version particularly, we use two cameras that are synchronized to ensure continuous recording of the state of the chain.

We find that the chain in these quasi-2D setups faithfully reproduces all key features and the different states we have reported [11], except that in our previous work the chain is vibrated along an open groove in 3D: at small values of Γ, the chain remains essentially flat; in a certain range of Γ, one end or both ends of the chain tend to dominate the movements; at even higher values of Γ, all particles are excited such that the movements no longer have a simple recognizable pattern. The scope of this work is to understand dynamics of the chain in the first two regimes.

Most strikingly, in the second regime, we find that the chain can *spontaneously* switch its state of excitation without the value of Γ ever changed, as demonstrated by Fig. 2. Here the motion is time-resolved within every vibration cycle, and we compute the variance of the height along the chain (by fitting its image with a smooth polynomial) to measure the degree of bending Δz^2 as a function of time. Fig. 2(a) uses Γ =1.65 as an example to show that, when active, $\Delta z^2(t)$ exhibits a maximum once every vibration cycle [12]. Interestingly, these peak values indicate that, over time, the chain switches back and forth between an *inactive* state (with Δz^2 always close to zero) and those *excited* state(s). Fig. 2(b) further characterizes this feature by the histogram of $\Delta z^2{}_{max}$ and a fitting with the superposition of two gaussians: a fraction formed by the fitting parameters establishes a degree of excitation that grows with Γ. For a wider range of Γ, Fig. 2(c) compares the 12-minute time average of the bending of the chain at different values of Γ, showing the gradual transition and a saturation.

Simple as they are, the statements above address neither the dynamics of spontaneous switching nor the distinctions between different states of excitation. In the following two sections, we establish tools for detailed analyses, from both microscopic and statistical point of views.

III. MICROSCOPIC ANALYSES

We track and analyze the motion of individual particles. Images of the chain are captured at high frame rates, with the center of individual particles determined by algorithms based on circle recognitions , giving a sensitivity at the order of O(10μm) [13].

A. Spontaneous switching of states

Figure 3 demonstrates the spontaneous switching at Γ = 1.65, among different states shown by the inset photographs. The heights and energies of the two end particles serve as good indicators for categorizing the response into State 0 (flat), State 1 (with one end active), and State 2 (with both ends active). The switching of states is typically within 10 vibration cycles, that is relatively abrupt in comparison to the persistent time of each state. The small curvature of the substrate might have shifted the reference height for the potential energy by the amount of 2mm but is not enough to wash out the abrupt changes among the different states. The on-and-off behaviors in kinetic energy are more obvious than that of the potential energy. However, we also note that the total energy is dominated by the change in potential energies, as the contributions from the kinetic energies (even for the most active particles at two ends) are relatively small. In terms of the long-time average, only State 0 is obviously lower than the other two states, for panel (e) shows that the switching from State 1 to 2 also evens out the rise of the two ends to a certain degree.

At higher frame rates, we are able to resolve the details of the switch from State 0 to State 1, as shown by Fig. 4. In State 0, panel (d) shows that all particles land on the substrate almost simultaneously within a relatively narrow time window denoted as A; many of them make a re-bounce and are identifiable with a second

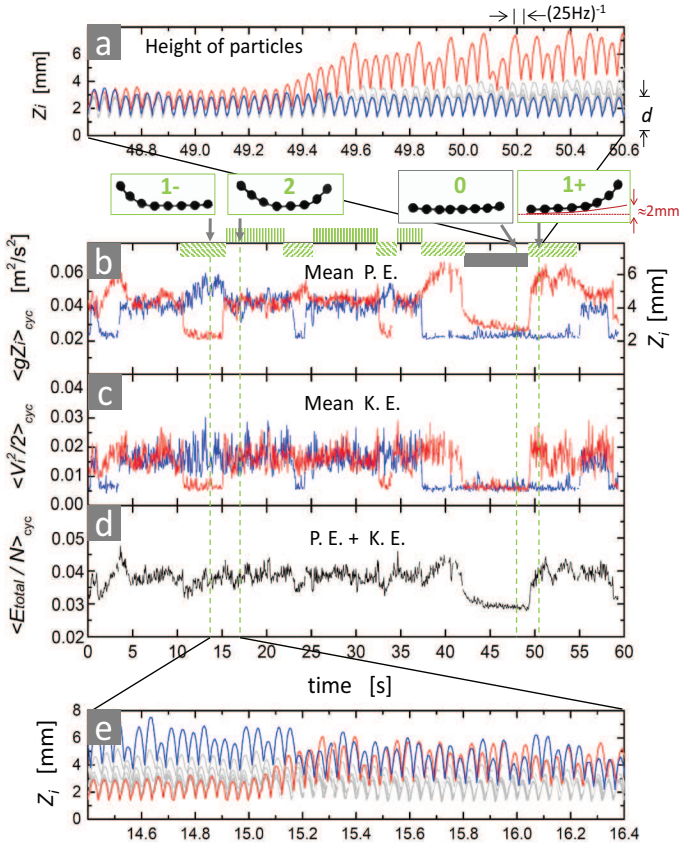

FIG. 3. Spontaneous switching of states at $\Gamma = 1.65$, 25Hz, $N = 8$ with setup $\alpha 2$. Images of different states upon their maximal bending are shown by inset photographs. Height of individual particles Z_i are time-resolved at 500fps in panel (a) and (e), demonstrating the transition from state 0 to 1, and 1 to 2, respectively. Two colors denote particles at two ends of the chain, while others are shown by light gray. Panel (b-c) show the potential energy gZ_i and kinetic energy $V_i/2$ of the end particles, averaged over each vibration cycle, while panel (d) shows the time evolution of the average energy along the chain, for a recording of 1 minute.

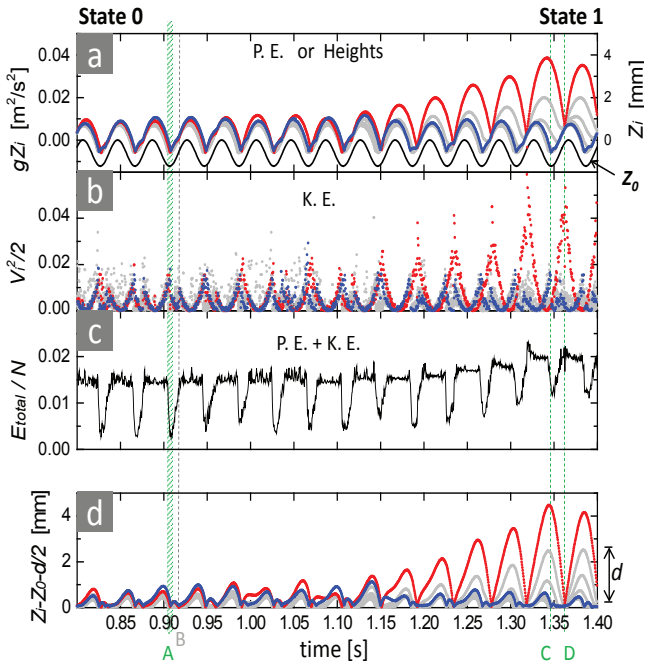

FIG. 4. Details of a switch from State 0 to 1 at $\Gamma = 1.65$, 25Hz, $N = 8$ with setup $\alpha 2$, captured at 2500fps. The heights and energies of individual particles are resolved within each vibration cycle in panel (a-c), while the movement of the substrate is displayed as Z_0. The separations of individual particles from the substrate are shown in panel (d). In State 0, the narrow time window within which particles land on the substrate is denoted as A; in many cases, a re-bounce with a second landing B is also visible. In State 1, symbol C indicates the strongly dissipative first contacts, in contrast to the ballistic bouncing of the end particle shown as D.

landing at B. On the other hand, State 1 has a significant spread in the time sequence of contacts: the interactions start with the strongly dissipative landing of many particles, marked as C, and finish with the ballistic impact of the end particle on the substrate, marked as D. Despite the dramatic difference in time sequence, we note that in both states the *total energy*, shown as in panel (c), dissipates quite abruptly upon the first landing (A or C) but its re-supply is relatively slow, made presumably by the upward movement of the substrate until the free flight starts (after B or D). The total energy then remains essentially unchanged (except with small fluctuations reflecting errors in our particle tracking) until the next landing. The implications of these interactions will be revisited after the discussion of a hypothetical point mass on a vibrating substrate.

B. Comparison to a point mass

To understand the interaction of an object with the substrate, it is helpful to consider a thought experiment with one point mass taking off from a substrate oscillating with $(\Gamma g/\omega^2)\cos\omega t$. Assuming that the point mass is non-cohesive and initially at rest on the substrate, elementary calculations reveal that this object leaves the plate at phase $\phi_{(0)} = -|\arccos(1/\Gamma)|$, makes a parabolic flight, and returns to the substrate at a phase $\phi_{(1)}$ that is also independent of the frequency ω [14].

The object may repeat this scenario indefinitely, but only if it has a zero restitution coefficient that dissipates all energy upon its landing. In reality, we have measured the re-bounce of one single particle dropped onto our substrate: the sample trajectories are shown in Fig. 5(c), giving a restitution coefficient and an estimated $e^2 \approx (0.50\pm0.04)^2 \approx 25$ percent of the energy left behind each collision.

Secondly, we track the re-bounce of particles along

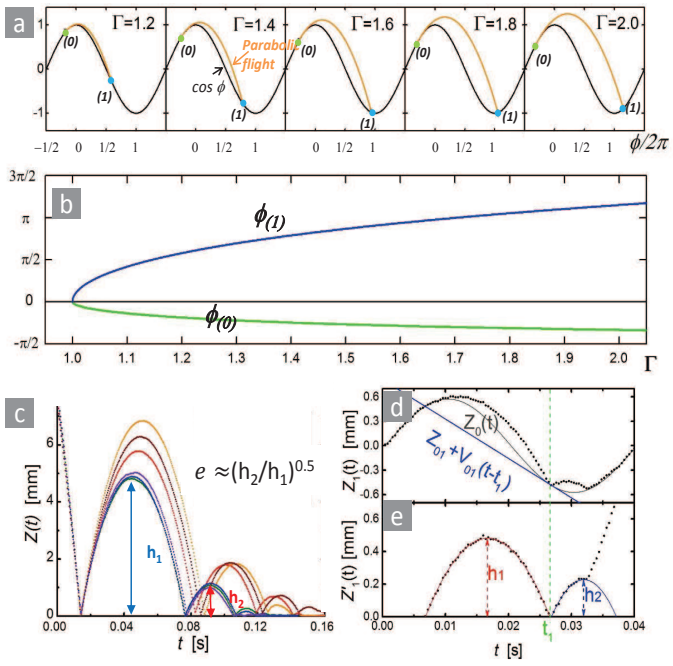

FIG. 5. Theory and empirical facts on the particle-substrate interaction. **(a-b)** The idealized parabolic flights of a point mass with no re-bounce, the phase $\phi_{(0)}$ for the take-off, and $\phi_{(1)}$ for the landing, as functions of the dimensionless vibration intensity Γ. The substrate oscillation, normalized by its amplitude, is set to be $\cos(\phi)$ with $\phi = \omega t$. **(c)** 6 empirical trajectories of single particles dropping onto our substrate, for assessing the restitution coefficient e. **(d)** Trajectory of one particle in a chain, $Z_1(t)$ in solid dots, the movement of the substrate $Z_0(t)$ in gray and its tangent upon the point of impact t_1, with Γ=1.45 at 25Hz with $N = 8$, setup $\alpha 2$. **(e)** Same trajectory as in (d) but in another inertial frame defined in main text, revealing two parabola equivalent to those in (c).

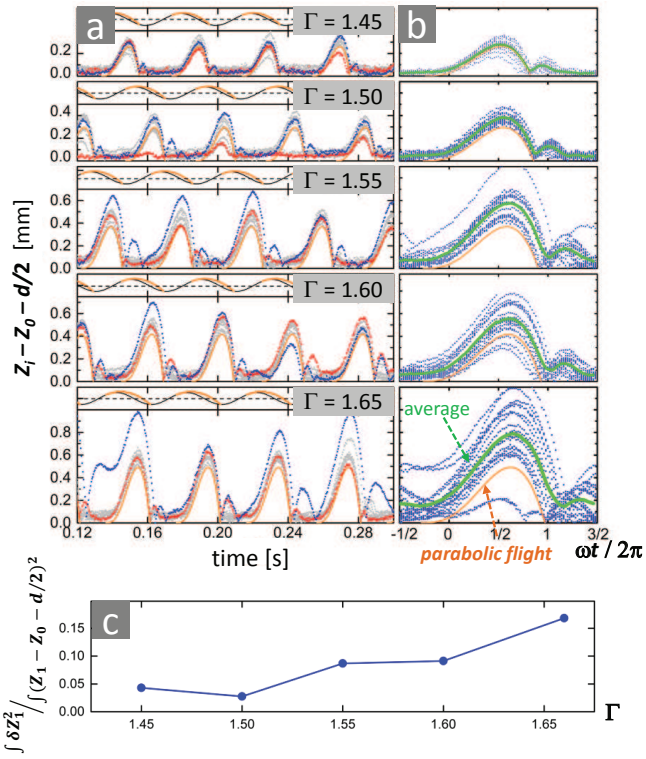

FIG. 6. Distance of individual particles from the substrate, as functions of time t, for different values of Γ. 25Hz, $N = 8$, in periods of State 0. **(a)** Sample trajectories, with the end particles displayed by two different colors and others in gray. The phase of the substrate and the hypothetical parabolic flight are also displayed above each sub-panels. **(b)** Trajectory of one particle accumulated from 18 vibration cycles, projected onto one single period. The thick line shows the average, with the hypothetical parabolic flight displayed by the thin line. **(c)** The variance among the trajectories shown in (b), $\delta Z_1{}^2$, normalized by the mean separation with the substrate over the entire cycle, as a function of Γ.

the chain with the vibrating substrate. Fig. 5(d) shows the trajectory of the end particle $Z_1(t)$ of one such re-bounce, while Fig. 5(e) shows the conversion to the inertial frame in which the point of impact appears static, $Z_1'(t) = Z_1(t) - (Z_{01} + V_{01}(t - t_1))$, and the fitting with two parabola for the purpose of deriving the restitution coefficient. The repetition of 12 vibrations gives a restitution coefficient $e \approx 0.55 \pm 0.07$, in consistence with that from the ball dropping experiment described above. However, as we shift our attention to particles away from both ends, we find significantly higher dissipations: For the third particle from one end of an eight-particle chain, about half of the impacts do not have a recognizable re-bounce; for the two particles closest to the center, only about 20 percent of the landings have an identifiable re-bounce, suggesting that at most 5 percent of the kinetic energy could survive the impact. The strong dissipation among these inner particles, estimated 95 percent, gives a plausible explanation on why the hypothetical model based on a fully dissipative point mass could mimic the overall behavior of State 0, even if the end particles may exhibit certain degree of re-bounces.

C. Precursor of transition

We observe the bouncing of particles at various vibration intensities. Fig 6 shows that, at Γ as small as 1.45, the scenarios are quite close to the bouncing of a fully dissipative point mass discussed previously, presumably because the kinetic energies are always fully dissipated before the next take-off. However, as Γ increases, we see not only clear deviations from the hypothetical curve, but also large variations among different cycles of vibration. Even if we deliberately choose to collect these data in the period of time that the chain remains apparently in "State 0" with no obvious rising of the end particles, the degrade of regularity with increasing Γ is evident, as shown quantitatively by the variation of trajectories

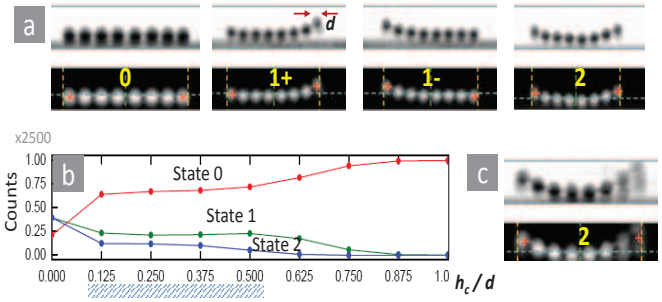

FIG. 7. Image-based definition of states – **(a)** Sample images and tracking results, with small crosses indicating the center of the first and last segments, the large cross showing the center of the middle particles. The long dashed line indicates the threshold height $h_c = d/4$ above the center of the middle particles, for defining the states. **(b)** The time fraction of each state for an accumulation of 2500 vibrations, using different choice of h_c. The results are insensitive to the change of h_c within the range marked by stripe. **(c)** Sample of an blurred frame and its result.

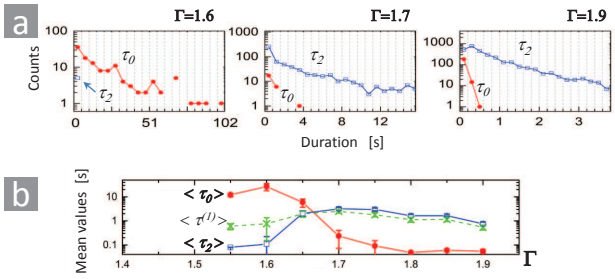

FIG. 8. Durations of events defined by the switch of states. $N = 8$, 25Hz, $h_c = d/4$, based on about 40 minutes of recording in setup β. **(a)** Histogram of the durations for State 0 and State 2, τ_0 and τ_2, with the bin width indicated by the vertical grid lines, at three different vibration intensity. **(b)** Mean values of τ_0, τ_2, and the average time for either end of the chain staying active $\tau^{(1)}$.

among different cycles. We regard the degrade as an interesting precursor of the *transition* to the dominance of those excited state(s), over the gradual increase of vibration intensity.

Combining the information from Fig. 4, Fig. 5, and Fig. 6 leads our understandings of the transition over Γ as follows. The strong dissipations inside the chain explain how State 0 could be maintained as the energies are repeated annihilated upon their landing, and the trajectories in Fig. 4 further reveal that, at $\Gamma \sim 1.65$, the chain repeatedly makes its landing at a phase very close to the *lowest* point of the vibration. This value is also consistent with the prediction from the hypothetical model presented as Fig. 5(a-b). However, this situation is inherently unstable, because the hypothetical model also suggests that any small stochastic delays on the parabolic flight would result to subsequent impacts with the substrate at its *rising* phase. There is a very good chance that the particles earn energies from these delayed impacts more than the dissipations along the chain, causing an accumulation of energy – and it is understandable that the accumulation is more likely at either end of the chain where the dissipation is lower. But for smaller values of Γ, the particles tend to hit the substrate at its falling phase that tends to absorb energy, and have relatively more time for the kinetic energies to fully dissipate before the next take-off. These provide a basic explanation on the transition over Γ, as we will investigate more with statistical characterizations.

IV. STATISTICAL DESCRIPTION OF TRANSITIONS

A. Image-based recognition of states and durations

To characterize the continuous transition over vibration intensity, we first introduce the circular channel, previously described as setup β, that allows unlimited observation time [15]. Influence of the small curvature is negligible, for that the expected bending to comply with the channel, if any, is only at the order of 10^{-2}radian between adjacent particles in average, and that this setup also reproduces all main features we have observed with the linear track. We deliberately use a low frame rate which matches that of the vibration, and utilize an *optical averaging*: that is, we set the exposure time to be close to the entire vibration period (0.04s, for instance). This way, we obtain the information from each entire cycle, without further efforts in synchronization techniques. More importantly, by analyzing these average images, we are able to establish an imaged-based recognition of states: the four states are defined by comparing height of the intensity-weighted center of the first or last $1/N$-th segment of the image, to that of the center segment. See photographs and the automated judgements shown in Fig. 7(a).

Although we have inevitably introduced a threshold h_c for criterion, we have also verified that the statistics are reasonably insensitive to the change of h_c for a certain range as shown by Fig. 7(b). Less than a few percent of the images are blurred presumably due to the occasional double collisions in one vibration. Nevertheless, the same algorithm still gives reasonable judgements of the state for those undesired images like Fig. 7(c).

The switching of states defined by the states specifies discrete *events*, with their durations shown in Fig. 8. These graphs demonstrate that as Γ increases from 1.6 to 1.7, the system undergoes a qualitative change from the dominance of long events of State 0, at the time scales

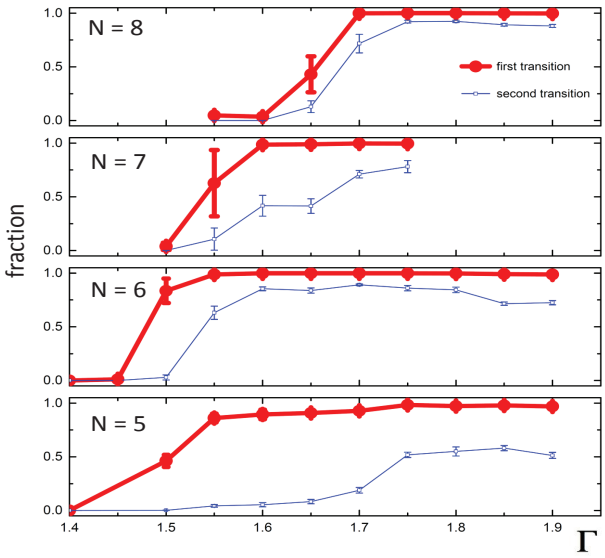

FIG. 9. Transition of behaviors over Γ, with different lengths of the chain. The first transition (away from the dominance of State 0, the thick line) is characterized by rise of the fraction of time that at least one end of the chain is determined to be active, while the second transition (to the dominance of State 2, the thin line) refers to the rise of both ends. (25Hz, accumulation of 40 minutes of data on setup β, $h_c = d/4$)

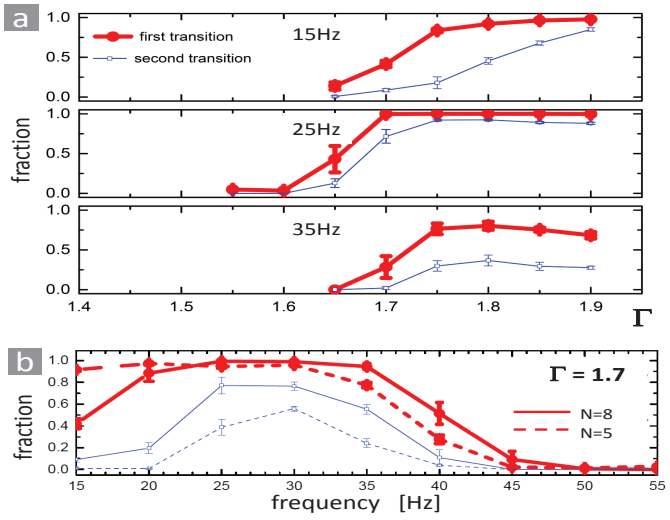

FIG. 10. Statistical observations at three different frequencies — thick lines mark the the first transition and thin lines the second, based on 40 minutes of data accumulated on setup β; $h_c = d/4$. **(a)** Transitions over Γ at three different frequecies; $N = 8$. **(b)** Comparison between two different lengths of chain, $N = 8$ (solid lines) and $N = 5$ (dashed lines), at Γ =1.7

of 10s, to a wide spectrum of short events of end swinging, at the time scale of 1s. The distributions are clearly not exponential, suggesting that the states have certain memory, as one may also perceive from our previous microscopic analyses.

B. Time fraction: dependence on chain length

The automated image recognition provides many convenient tools for assessing the role of various factors on the transition over Γ, based on long-time statistics. One example is to use the fraction of time during a long recording as a representation of the "probability" that the chain chooses to be in specific states, thus we characterize the *first transition* by the rise of the such probability over the increase of Γ that at least one end of the chain is determined as active, and a *second transition* by the activation of both ends — see the thick line and thin line in Fig. 9, respectively. The data present the effect of chain length N on the transition and show that the decrease of chain length in general makes the first transition occur at lower values of Γ. We interpret this result as follows, based on our analyses and measurements of the re-bounce of particles along the chain discussed in Sec. III.B: a shorter chain is less dissipative and more energy survives the landing impacts. It is then not surprising that its behavior would deviate more from the prediction of a fully dissipative point mass, and that the crossover from State 0 to State 1 tends to occur at lower values of Γ.

We also note that, for a chain as short as $N = 5$, the second transition seems to occur with a much larger lag along the change of Γ than the first transition, in comparison to the cases with longer chains. We believe that this suggests a length-scale below which the two ends of the chain can no longer be seen as independent: activation of one end of a five-particle chain somehow hinders the energy accumulation at the other. Further investigations are needed to confirm this conjecture.

V. DISCUSSIONS

The combination of microscopic and statistical tools allows the discussions on the role of different factors, such as the frequency or amplitude of the substrate, behind these phenomena.

A. Role of frequency

Using time fractions as convenient indicators of transition, Fig. 10 presents our assessment on the role of frequency in our experiments. Panel (a) shows that the system exhibits similar trend with the change of Γ at three different frequencies, except that the first transition seems incomplete in the case of 35Hz: its statistics show a finite fraction of time in which both ends of the chain are determined as inactive. Whether the incompleteness stands for an artefact due to our use of a thresh-

old scale $h_c = d/4$ in state criterion, or as an indication that the transition does vanish at higher frequencies, is so far inclusive, partly because of the dramatic decrease (to the inverse square of frequency) in the spatial scale of response which, in the case of 45Hz, already drops below our current accuracy for reliable determination of the state of the chain from the averaged images. We will have further comments on the issue of small amplitudes in the next subsection.

On the other hand, our current instrumentation prevents us from determining whether the head-swinging phenomena would sustain at the low-frequency limit. However, we believe that such scenario is unlikely, because the kinetic energy at either end of the chain is likely to be dissipated in finite time so that it is hard to imagine that such accumulation could sustain for an indefinitely long period of vibration [16]. Estimating such time scale, based on the experimental information we have provided, could be an interesting theoretical problem.

Phenomenologically, we have identified an optimal window of frequency from 20 to 30 Hz for observing the transitions with the current setup and materials at hands. We do not believe the end-swinging as some kind of mechanical resonance, because such resonance is expected to be sensitive to chain length but the data in Fig. 10(b), with N varied by almost a factor of two, suggest otherwise.

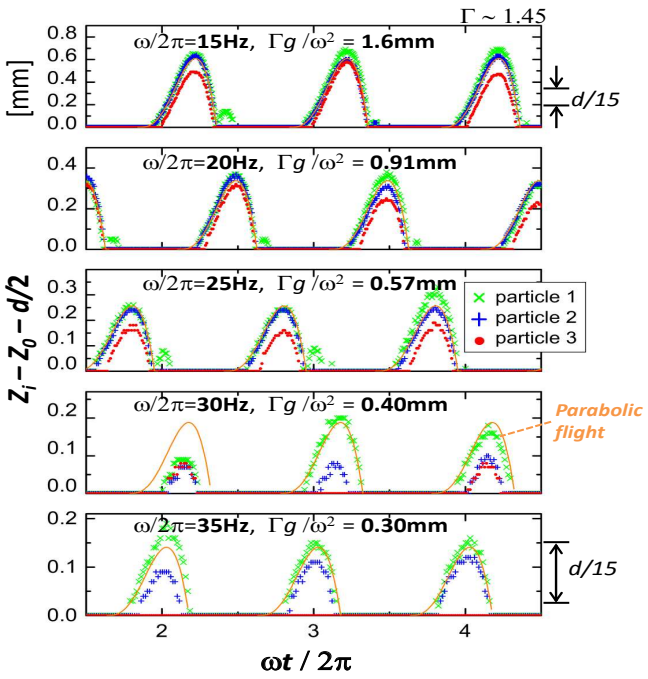

FIG. 11. Trajectories of three of the particles in a chain with $N = 8$ at State 0, at the vibration intensity around 1.45, showing clear deviations from the hypothetical parabolic flight and increasingly complicated behaviors, as results of the smaller amplitudes.

B. Complications at small amplitudes

In a fixed range of Γ, the spatial amplitude of vibration decreases as the inverse square of the frequency as it increases. What if the vibration amplitude becomes much smaller than the size of the particles?

Figure 11 demonstrates the potential complications associated with the decrease of amplitudes. With a similar value of Γ ∼1.45, we observe trajectories of three of the particles in the chain at the simplest State 0. As we increase the frequency towards 35Hz, the amplitude $\Gamma g/\omega^2$ decreases to 0.3mm: the expected flight of a hypothetical particle would be at the order of 0.15mm or about $\frac{1}{15}$ of a particle diameter only — it seems unlikely that the oscillatory driving at such a small spatial amplitude can be rectified into a significant bending along the chain at the order of particle size. We believe that the response to such small amplitudes can be sensitive to any imperfections (the asymmetry of the spheres or dirts) or the connecting mechanisms. And indeed, as the amplitude decreases, the data show not only obvious deviations from the prediction of the hypothetical point mass, but also other signs of complications that particles can appear to stick to the substrate sometimes. These factors also contribute to reasons why we tend to be conservative in interpreting our statistics at higher frequencies, other than just the limitations on image resolutions.

Despite these complications, it is worth mentioning that the steady creeping of the ground state (referred to as State 0 here) in our previous work with a spatial gradient of excitation sustains at extremely small amplitudes of vibration – down to those associated with 70Hz or smaller than $\frac{1}{60}$ of the particle diameter in terms of the spatial scale. We believe that this steady creeping must be underlined by more generic reasons that do not depend on the exact details in the movements of individual spheres.

VI. CONCLUSION

In this work, we systematically study the behaviors of a short granular chain in response to a uniform but tunable intensity of vibration. The quasi-2D setup reproduces the multiple states and transitions that we previously discovered on open channels in 3D . In certain ranges of excitation intensity, the chain exhibits spontaneous switching among different states at a fixed intensity of vibration. This coexistence of possibilities in different states explains why in our previous work with a spatial gradient of excitation [11] we see qualitatively different bouncing modes occur at the same initial position and, in turn, create the dramatic spatial divide under suitable conditions. We use two sets of strategies to characterize the bifurcation of states and the transition over vibration intensity Γ. Time-resolved tracking of individual particles, with high-speed imaging, measures the energies and

details on the interactions with the vibrating substrate. Statistical analyses on the long series of images, time-averaged over each vibration cycle, provide quantitative descriptions of the transitions over Γ and help us understand the role of various factors behind the transition, such as the length of the chain.

Consideration of the parabolic flight of a hypothetical point mass is a helpful starting point for understanding the bifurcation that leads to the transition over Γ. However, a few questions remain answered: What determines the length of the chain below which the behaviors change qualitatively? And what are the complete set of conditions for the instability leading to the accumulation of energy towards the end of the chain? In addition, our experiments offer several specific targets for analytical or numerical studies. Other than the scale-independent steady creeping of ground state in our previous work that demands an explanation, the interplay between the driving amplitude and the scale of the particles also calls for further understanding. Should the bending of the chain also scale with the spatial amplitude of the vibration, so that the uniform bouncing would be the only permissible scenario at the high-frequency limit? Can one establish a *minimal model* for the competition between the dissipation and the accumulation of energy along the chain, in order to predict a lower bound in frequency for the end-swinging to be observed? We believe that these problems help elucidate how, in general, the internal degrees of freedom of a soft object interact with external driving in exchanges of energy and momentum and, in turn, affects its macroscopic motion.

* JC Tsai <jctsai@phys.sinica.edu.tw>
† JR Huang <jrhuang@ntnu.edu.tw>

The authors acknowledge fruitful exchanges with M.-R. Chou, C.-Y. Tao, F.-Y. Chang, C.-K. Chan, assistance from AS-IoP Machine Shop, and funding support from AS-IoP and MoST in Taipei, Taiwan.

[1] Yamada, T. Hondou, and M. Sano, Phys. Rev. E 67, 040301 (2003).
[2] S. Dorbolo, D. Volfson, L. Tsimring, and A. Kudrolli, Phys. Rev. Lett. 95, 044101 (2005); D. Volfson, A. Kudrolli, and L. S. Tsimring, Phys. Rev. E 70, 051312 (2004).
[3] J. Atwell and J. S. Olafsen, Phys. Rev. E 71, 062301 (2005).
[4] P. M. Reis, R. A. Ingale, and M. D. Shattuck, Phys. Rev. E 75, 051311 (2007).
[5] H. S. Wright, M. R. Swift, and P. J. King, EPL 81, 14002 (2008).
[6] R. d. Wildman, J. Beecham, and T. l. Freeman, The European Physical Journal Special Topics 179, 5 (2009).
[7] J. J. Barroso, M. V. Carneiro, and E. E. N. Macau, Phys. Rev. E 79, 026206 (2009).
[8] K. Jiang, P. C. Thomas, S. P. Forry, D. L. DeVoe, and S. R. Raghavan, Soft Matter 8, 923 (2012).
[9] Y. Kubo, S. Inagaki, M. Ichikawa, and K. Yoshikawa, Phys. Rev. E 91, 052905 (2015).
[10] See also V. Yadav and A. Kudrolli, The European Physical Journal E 35 (2012) and A. Kudrolli, Phys. Rev. Lett. 104, 088001 (2010) for experiments with short chains of beads interacting with others. The discussions, however, are mainly on the lateral movements rather than on the state of the objects.
[11] W.-T. Lin, Y.-C. Sun, C.-C. Chang, Y.-C. Lin, C.-W. Peng, W.-T. Juan, and J.-C. Tsai, Phys. Rev. Lett. 112, 058001 (2014).
[12] See also videos clips on the Online Supplements http://www.phys.sinica.edu.tw/jctsai/GPT2015/ for additional evidence that the chain actually leaves the substrate once every cycle, and that the maximum occurs very close to the moment when the chain falls back to the substrate.
[13] Y.-C. Sun, *Master Thesis*, National Taiwan Normal University, June 2015, Taipei, Taiwan. Also available through our Online Supplements.
[14] $\phi_{(1)}$ can be solved numerically from $\Gamma\cos\phi_1 = 1 - \sqrt{\Gamma^2-1}\cdot(\phi_1 - \arccos(1/\Gamma)) - (\phi_1 - \arccos(1/\Gamma))^2$. See also the *Master Thesis* for details.
[15] In addition to vertical bouncing, the chain often exhibits considerable movements in the horizontal direction. With a linear track, statistical analyses could either be hindered by the limited time span (with setup $\alpha 1$) or be somewhat biased as the chain drifts along the slightly concave bottom (with setup $\alpha 2$). The use of a circular channel removes such constraints. Further observations and analyses, on the interplay between the states of the chain and its horizontal motion, will be covered in our subsequent publication.
[16] Up to the submission of this manuscript, we have found that, at 10Hz, an eight-particle chain indeed stays in State 0 and shows no signs of transition within the current scope of discussion $1.4 < \Gamma < 2.0$.